

The Structure of a Human Voltage-Gated Potassium Kv10.2 Channel which Lacks a Cytoplasmic PAS Domain

G. S. Glukhov^a, A. V. Popinako^b, A. V. Grizel^c, K. V. Shaitan^{a, d, *}, and O. S. Sokolova^a

^aMoscow State University, Moscow, 119991 Russia

^bResearch Center of Biotechnology, Russian Academy of Sciences, Leninskyi pr. 33/2, Moscow, 119071 Russia

^cSt. Petersburg State University, Universitetskaya naberezhnaya 7/9, St. Petersburg, 199034 Russia

^dSemenov Institute of Chemical Physics, Russian Academy of Sciences, ul. Kosygina 4, Moscow, 119991 Russia

*e-mail: shaitan49@yandex.ru

Received April 18, 2016

Abstract—The three-dimensional structure of a human voltage-gated potassium Kv10.2 channel which lacks a cytoplasmic *N*-terminal PAS-domain was determined, and its distribution in eukaryotic cells was investigated. The channel protein was expressed in the *COS7* cell line and purified by affinity chromatography. The channel distribution on the cell surface was determined by the immunofluorescence method using the antibodies against its *C*-terminus. PAS-domain truncation was shown to cause a decrease the expression of the channels on the cell surface. In order to reveal the positions of the channel cytoplasmic domains, the three-dimensional structure of the protein lacking the cytoplasmic PAS-domain was compared to the previously obtained full-length structure. We demonstrated that the *C*-terminal CNBD-domain of the Kv10.2 channel undergoes conformational rearrangements in the absence of its *N*-terminal PAS-domain.

Keywords: ion channel, electron microscopy, three-dimensional protein structure

DOI: 10.1134/S0006350916040102

INTRODUCTION

Ion channels are responsible for the electrical activity in different cell types. They have been found in all human tissues and organs and are predominantly present in the central nervous system, heart, and muscles. The number of described ion channels increases every year. The structure of ion channels may vary in different tissues and variations in molecular structure and pharmacological properties of certain ion channels lead to an increase in the overall number of their subtypes.

Kv1 (*Shaker*), Kv2 (*Shab*), Kv4 (*Shal*), Kv7 (KVLOQ), and Kv10–12 (*Ether-a-go-go*) [1] represent the most studied families of voltage-gated potassium (Kv) channels. Kv channels are characterized by a similar molecular architecture: they are tetramers in which each subunit contains six transmembrane regions, S1–S6, including the membrane potential sensor, S4 [2].

The *Ether-a-go-go* subfamily (Kv10–12) is characterized by the presence of prolonged *N*- and *C*-terminal sequences that are organized in several structural domains. The PAS-domain (Per–Arnt–Sim), which is composed of 135 amino-acid residues, is located at the *N*-terminus of the channel. The domain is responsible for the activation of the channel [3, 4], and for modulation of its inactivation, possibly due to direct

binding to the site adjacent to the linker region, S4–S5 [5–8]. The crystal structure of the *herg* (Kv11) channel PAS-domain has been resolved [5].

The cyclic nucleotide-binding domain (cNBD) is localized at the *C*-terminus of the channel. This domain has also been identified in different unrelated channels: namely, in plant potassium ATK and KAT channels and cyclic nucleotide-dependent (HCN) channels that are activated by hyperpolarization. Recently, the crystal structures of the cNBD-domains in HCN [9] and HCN1 [10] channels were published. Deletion of the *C*-terminus was shown to result in a loss of Kv channel function.

We previously determined the three-dimensional (3D) structure of the full-length Kv10.2 channel using electron microscopy [11] and demonstrated that the large cytoplasmic domain of each monomer is composed of two subdomains. The goal of the present study was to identify the positions of the PAS- and CNBD-domains in the channel and to elucidate their functions during channel expression in eukaryotic cells.

METHODS

Preparation of DNA encoding a truncated channel protein. We used the *DH5 α* strain for plasmid develop-

ment. Isolation of plasmids for transient transfection of eukaryotic cells was carried out using the standard method of alkaline cell lysis [12]. The actual plasmid concentration for transformation was equal to 5–9 $\mu\text{g}/\mu\text{L}$.

Expression and purification of the truncated channel. The eukaryotic *COS7* cell line was used for transient expression of the potassium Kv10.2 Δ PAS channel. Cells were grown on Petri dishes in a DMEM high glucose medium (HyClone, United States) that contained 10% fetal bovine serum. Cells were transfected with pcDNA6 5V-his plasmids, which encode the Kv10.2 channel lacking the PAS-domain via electroporation on a Gene Pulser Xcell (BioRad, United States), in accordance with the manufacturer's instructions. The final plasmid concentration was 50 mg/mL.

After transfection, the cells were cultivated for 48 hours. The cells were then washed with cold phosphate buffer saline and treated by a lysis buffer (20 mM HEPES, 2.5% CHAPS). All procedures were carried out on ice or at 4°C in the presence of protease inhibitors (Roche, Switzerland). Protein purification was carried out with the use of affinity chromatography on a BrCN-activated agarose coupled with anti-1D4 antibodies, as previously described [11]. Protein elution was performed with a 1D4 peptide (American-Peptide, United States) diluted to the concentration of 2 mg/mL. The channel protein concentration in a sample was determined by Western blotting with anti-1D4 antibodies (Abcam, Great Britain).

Fluorescent microscopy. After electroporation, the cells were grown on round 24-mm glass cover slips in six-well plates ($1 \cdot 10^6$ cells per well) for 22–24 h in 2 mL of DMEM high glucose medium containing 10% fetal bovine serum. 24 h after transfection, the culture medium was refreshed and the cells were incubated for an additional 24 h. The cells were fixed in 2% paraformaldehyde, and permeabilized with a 0.1% Triton X-100 solution. Anti-1D4 antibodies were used as primary antibodies, while secondary antibodies were labeled with AlexaFluor 488 (Abcam, Great Britain). The fluorescence signal was detected using an Axio Lab.A1 fluorescent microscope (Zeiss, Germany) equipped with a CCD camera (Nikon, Japan). Images were analyzed using the ImageJ software (<https://imagej.nih.gov>).

Single particle electron microscopy. 3 μL of purified channel protein was immediately put on electron microscopy grids coated with a carbon film, subjected to negative glow-discharging in an air atmosphere and stained on drops (40 μL) of 1% uranyl acetate solution twice for 30 s each time.

Images of Kv10.2 Δ PAS were obtained using a JEOL 2100 electron microscope (JEOL, Japan) under an accelerating voltage of 200 kV. The images were registered with a CCD camera (Gatan, United States)

with a magnification of 40000 and a defocus of 1.4–1.9 μm .

Selection of images of single channels was made in a semiautomatic manner using the BOXER software [13]. For this purpose, a 64×64 pixel square that contained a channel projection was cut out of the electron microphotograph for each particle. In total, 4000 images of the Kv10.2 Δ PAS channel were selected. Images were filtered of noise, normalized, centered, and then classified using the EMAN2 software [13]. Each class contained channel images with the same orientation. Their summation led to an increase of signal-to-noise ratio. An angular reconstruction was used to calculate the initial tertiary structure using best class-sum images, which included many aligned channel particles [14].

Next, the two-dimensional back-projections of the preliminary 3D reconstruction were obtained, each of which possesses the same orientation as the corresponding class used to calculate the 3D structure. This resulted in an identical number of back-projections and classes used for the reconstruction. The back-projections were later used as new references for further particle alignment. Since four-fold symmetry of class-sum averages was detected, this type of symmetry was used for the calculation of the final 3D structure.

Homology-based modeling. In order to analyze the 3D structure of the truncated channel, we used atomic models of single domains, obtained by homology-based modeling. The crystal structure of the bacterial cAMP-dependent MloK1 channel (the PDB accession number is 2KXL) was used as a template for the transmembrane domain. The SWISS-MODEL server was used for the identification of templates [15]. Amino-acid sequences were aligned using the T-COFFEE software [16]. Based on homologous amino-acid sequence alignments, models were constructed using the MODELER software [17]. Models of the tetrameric structure were constructed taking into account the symmetry matrix, using the UCSF Chimera software [18]. The parameters of the symmetry matrix in the pdb file of the model were chosen in accordance with homologous proteins. Fitting of the models was performed in the semi-automatic mode with the Situs software [19].

RESULTS AND DISCUSSION

Voltage-gated potassium (Kv) channels represent an extremely widely distributed diverse group of proteins that perform important functions in animals, including humans. Kv channels may be considered as potential therapeutic targets for the treatment of a variety of diseases [20]. Presently, little is known about their quaternary structure due to difficulties in the preparation, purification, and crystallization of membrane proteins that possess large cytoplasmic regions. At the same time, structural data have primary signif-



Fig. 1. A schematic presentation of the Kv10.2 channel monomer. The following domains are indicated: PAS-domain, cNBD-domain, and the transmembrane region, whose segments are designated as S1 to S6.

importance for studying the mechanisms of channel functioning and activation and for de-novo drug design. The cytoplasmic parts of Kv-channels play an important role in regulation of the functioning of the entire molecule and provide major differences between channel families. The Kv10.2 channel is characterized by an especially large cytoplasmic part [11]. The polypeptide chain of its full-length α -subunit (Fig. 1) consists of 988 amino-acid residues with an approximate molecular weight of 120 kDa. The PAS-domain is composed of approximately 100 amino-acids (residues 31–132). The channel membrane part consists of six transmembrane segments, S1–S6, which are formed by residues from 144 to 550, while its C-terminus contains a CNBD domain that is formed by 118 amino-acid residues and, similarly to the N-terminal PAS-domain, is exposed to the cytoplasm.

The major function of Kv channels is the transfer of potassium ions across the cell membrane. Thus, in the cell, the newly synthesized channels should be delivered to the cytoplasmic membrane; this process is controlled by certain intracellular mechanisms [21]. Studies of the channels by fluorescent microscopy using labeled antibodies against the C-terminal 1D4 tag revealed that the voltage-gated Kv1.1 channel (*Shaker*) is expressed on the COS7 cell membrane at rather high densities. Figure 2a depicts a densitogram that shows that channels form multiple small clusters with diameters less than 0.5 μm . Additionally, there are multiple non-clustered channels in the membrane that form a dense background in the densitogram. These channels are active and perform their function to conduct potassium ions across the membrane, as we have previously shown [22, 23].

Kv10.2 channels form clusters in the cell membrane that are 0.5 to 1.0 μm in diameter (Fig. 2c). This is consistent with our data that were previously obtained [24] using labeled toxin. Unlike the full-length channels, the truncated Kv10.2 Δ PAS channel forms a small number of large (up to 2 μm in diameter) clusters that are located at large distances from each other (Fig. 2b). The fluorescence signal was not detected between the clusters, indicating that PAS-domain deletion caused the loss of the free active channels in the cell membrane.

It was previously suggested that the clusters are a deposit of inactive channels; they may dissipate into a great number of active channels as a result of decrease in the frequency of the action potential [25]. Thus, deletion of the cytoplasmic PAS-domain leads to inactivation of the channels by causing their clusteri-

zation. Furthermore, PAS-domain deletion may influence the transportation of the channel to the cell membrane.

As a result of the expression and purification procedures, a sufficient amount of purified Kv10.2 Δ PAS protein was obtained; its structure was studied by single particle electron microscopy with negative staining. To determine the 3D structure of the channel using electron microscopy, the purified protein was put on a grid and stained with a 1% uranyl acetate aqueous solution, as described in the Methods section.

The 3D structure of the protein was obtained using electron microscopy and image processing at a resolution of 22 \AA and is depicted in Fig. 3. The analysis of this structure revealed the presence of a transmembrane domain with dimensions of $10 \times 10 \times 5 \text{ nm}$ and a cytoplasmic domain with dimensions of $12 \times 12 \times 5 \text{ nm}$.

Previously, we reported the 3D structure of the full-length Kv10.2 channel [11] and demonstrated the interactions between its cytoplasmic PAS- and CNBD-domains. We also showed the arrangement of CNBD-domains in the full-length channel to be different from their position in the crystal structure. In the present study, in order to determine the localization of the cytoplasmic domains, we obtained a structure of the channel lacking the PAS-domains. Since, unlike in the Kv1-4 channel families, the N-terminal PAS-domains of Kv10 channels do not perform the tetramerization function [5], removal of these domains did not cause disorders in the tetrameric structure of the channel and allowed purification of the protein with the use of the C-terminal affinity tag.

Comparison of the obtained 3D structure of the truncated Kv10.2 Δ PAS channel (Fig. 3) to the full-length channel structure [11] revealed different localization of the cytoplasmic domains. Deletion of the N-terminal PAS-domain caused a shift of the cytoplasmic CNBD-domains to the channel periphery and alteration of the overall shape of the reconstruction. Docking of the CNBD-domain, obtained by homology modeling using the crystal structure of the HCN4 domain of the cAMP-dependent channel (PDB accession number 3OTF) into the truncated channel reconstruction demonstrated good agreement (Fig. 3). Unlike the full-length channel, cytoplasmic domains do not form a continuous ‘belt’ in the truncated channel. Separate domains in the truncated channel are linked via a central cavity localized on the channel symmetry axis. Previously, we observed a similar central density in the full-length channel

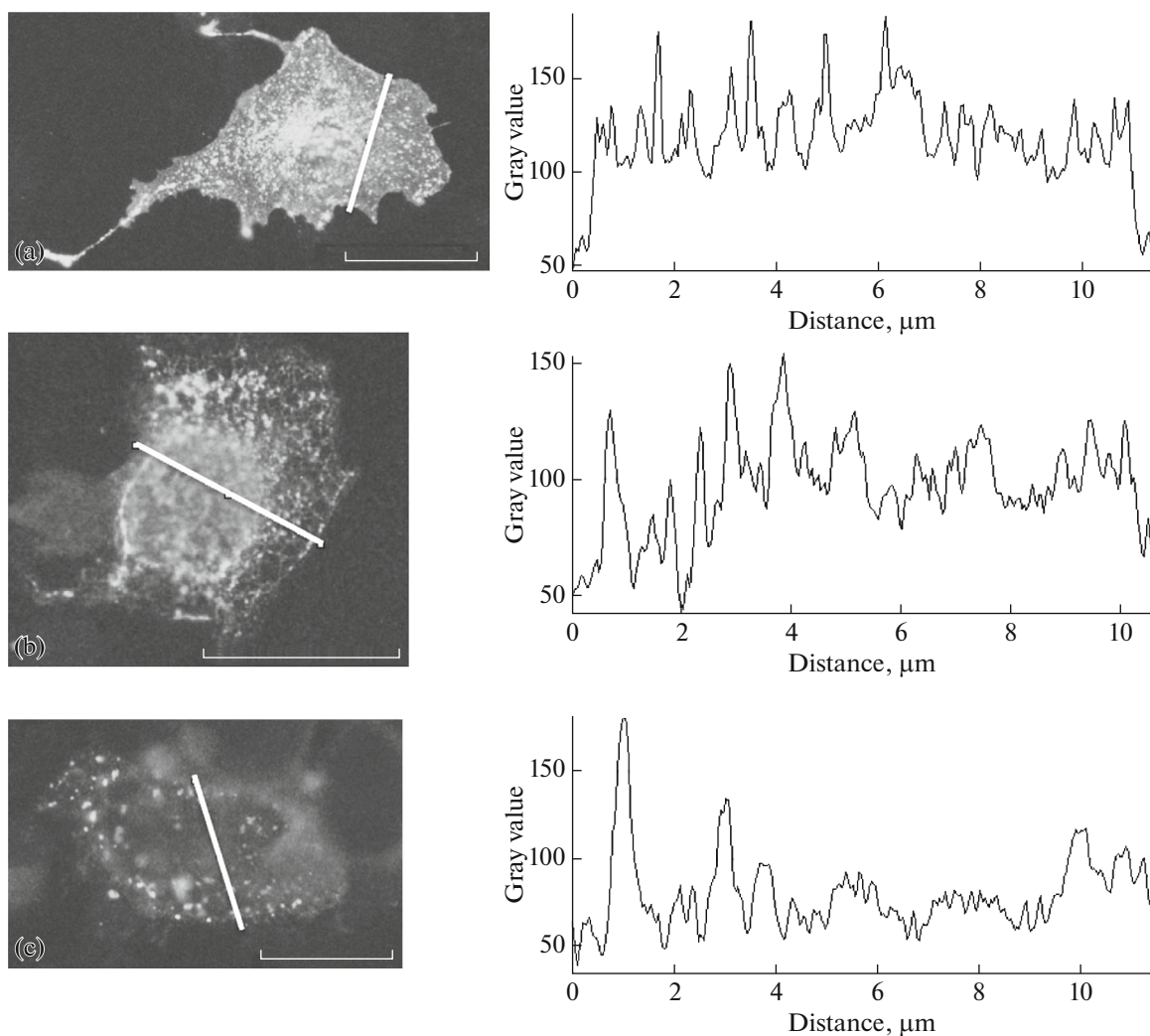


Fig. 2. The expression of ion channels in eukaryotic cells. The fluorescence images of channels labeled by antibodies against the C-terminal 1D4 tag (on the left). Intensity profiles are along the white line that crosses the image (on the right). (a) Kv1.1 channel (Shaker), (b) Kv10.2 channel, (c) Kv10.2 Δ PAS channel. The scale bar is 10 μ m.

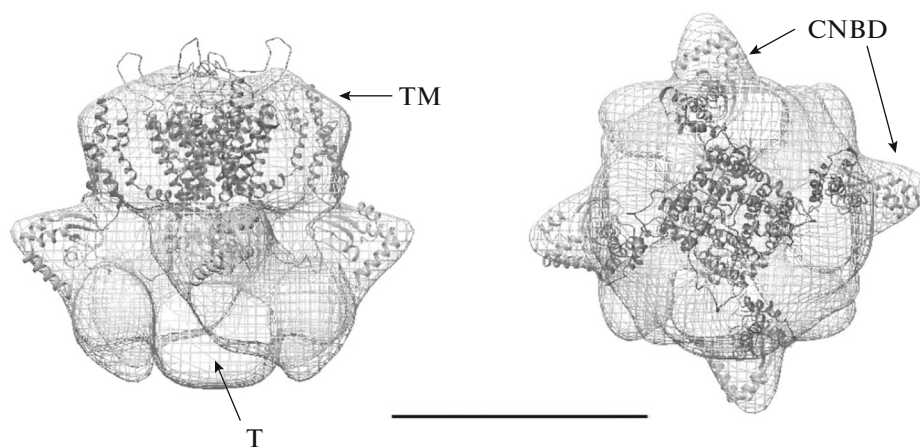


Fig. 3. The interpretation of the tertiary structure of the Kv10.2 Δ PAS channel by fitting the transmembrane domain model into the upper part of the channel reconstruction (dark grey) and cNBD-domains (light grey) within the cytoplasmic part of the reconstruction: (a) view from side, transmembrane domain (TM) and tetramerization domain (T) are indicated; (b) view from the transmembrane domain, CNBD-domains are indicated. The scale bar is 10 nm.

reconstruction [11]. The tetramerization CAD domain is known to be located at the C-terminus of the Kv10 channel. Deletion of this domain resulted in the synthesis of a non-functional channel [9]. We suggested that the central density remaining after deletion of N-terminal domain is the C-terminal tetramerization domain (designated as “T” in Fig. 3a).

Thus, in the absence of the N-terminal domain, the C-terminal domain of the Kv10.2 channel undergoes significant conformational rearrangements and moves to a position corresponding to the monomeric state of the CNBD-domain. The C-terminal CAD-domain of the Kv10 channel is responsible for the tetramerization function [9]. Besides, we showed that removal of the cytoplasmic N-terminal domain leads to changes in the expression of the channel on the cell surface and causes channel clusterization, which indicates that the function is carried out by a sequence located at the C-terminal of the Kv10 channel.

ACKNOWLEDGMENTS

The authors are grateful to I.A. Demyanenko and E.S. Trifonova for assistance in editing the manuscript. Electron microscopy studies were performed at the laboratory of electron microscopy of Department of Biology at Moscow State University.

This work was supported by the Ministry of Education and Science of Russian Federation (project ID: RFMEFI61615X0044). The JEOL 2100 electron microscope was purchased under the Moscow State University Development Program.

REFERENCES

1. F. H. Yu, et al., *Pharmacol. Rev.* **57** (4), 387 (2005).
2. G. Yellen, *Nature* **419** (6902), 35 (2002).
3. D. Wray, *Eur. Biophys. J.* **38** (3), 271 (2009).
4. D. Wray, *Eur. Biophys. J.* **38** (3), 285 (2009).
5. J. H. Morais Cabral, et al., *Cell* **95** (5), 649 (1998).
6. Z. Wang, G. F. Wilson, and L. C. Griffith, *J. Biol. Chem.* **277** (27), 24022 (2002).
7. L. Restier, L. Cheng, and M. C. Sanguinetti, *J. Physiol.* **586** (17), 4179 (2008).
8. H. Terlau, et al., *J. Physiol.* **502** (3), 537 (1997).
9. W. N. Zagotta, et al., *Nature* **425** (6954), 200 (2003).
10. M. Lolicato, et al., *J. Biol. Chem.* **286** (52), 44811 (2011).
11. O. S. Sokolova, K. V. Shaitan, A. V. Grizel, et al., *Russ. J. Bioorg. Chem.* **38** (2), 152 (2012).
12. H. C. Birnboim and J. Doly, *Nucleic Acids Res.* **7** (6), 1513 (1979).
13. S. J. Ludtke, P. R. Baldwin, and W. Chiu, *J. Struct. Biol.* **128** (1), 82 (1999).
14. M. van Heel, *Ultramicroscopy* **21**, 111 (1987).
15. F. Kiefer, et al., *Nucleic Acids Res* **37** (Database Issue), D387 (2009).
16. C. Notredame, D. G. Higgins, and J. Heringa, *J. Mol. Biol.* **302** (1), 205 (2000).
17. N. Eswar, B. Webb, M. A. Marti-Renom, et al., in *Current Protocols in Bioinformatics*, Ed. by A. D. Baxevanis et al. (Wiley, Hoboken, NJ, 2006), Unit 5.6.
18. T. D. Goddard, C. C. Huang, and T. E. Ferrin, *J. Struct. Biol.* **157** (1), 281 (2007).
19. W. Wriggers, R. A. Milligan, and J. A. McCammon, *J. Struct. Biol.* **125** (2–3), 185 (1999).
20. A. V. Pischalnikova and O. S. Sokolova, *J. Neuroimmune Pharmacol.* **4** (1), 71 (2009).
21. H. Misonou and J. S. Trimmer, *Crit. Rev. Biochem. Mol. Biol.* **39** (3), 125 (2004).
22. O. Sokolova, et al., *Proc. Natl. Acad. Sci. USA.* **100** (22), 12607 (2003).
23. O. Sokolova, L. Kolmakova-Partensky, and N. Grigorieff, *Structure* **9** (3), 215 (2001).
24. M. G. Karlova, et al., *Biofizika*, **56** (2), 272 (2011).
25. H. Misonou, D. P. Mohapatra, and J. S. Trimmer, *Neurotoxicology* **26** (5), 743 (2005).